Journal of Coastal Conservation (2023) 27:28
https://doi.org/10.1007/s11852-023-00955-x

Flood vulnerability under sea level rise for a coastal community located in a backbarrier environment, Portugal

Raphaelle Croteau[1] · **André Pacheco**[1] · **Óscar Ferreira**[1]

Received: 25 March 2023 / Revised: 10 June 2023 / Accepted: 20 June 2023 / Published online: 17 July 2023

Abstract
Sea level rise will be a major threat to coastal communities within the next century due to the intensity and severity of the floods it can cause. A new methodology considering water infiltration, slope, and hydraulic connectivity was developed to assess the potential inundation extension associated with different total water level and sea level rise scenarios on sandy coasts. This methodology was applied for the current conditions as well as 2050 and 2100 scenarios of storm surge and high tide levels with return periods of 1 year and 100 years. The study area is Culatra village, located on the lagoon side of a barrier island in southern Portugal. The effects of shoreline evolution after the construction of a harbor and associated beach nourishment were also evaluated within the inundation scenarios. The results show that, within the study area, total water level variations caused by sea level rise have a greater influence on the inundation extension than shoreline retreat. The village appears to be safe for the current and 2050 total water level scenarios with a 1-year return period but would be highly affected by 100-year return periods, especially from 2050 onwards. This novel approach represents an improvement on more common flood mapping methods such as the bathtub approach and can be easily applied to other backbarrier environments under sea level rise or facing coastal erosion.

Keywords Coastal hazards · Inundation · Coastal management · Sea level rise · Shoreline evolution

Introduction

One of the main consequences of climate change is sea level rise (SLR) which is mostly caused by increasing ocean temperatures (inducing thermal expansion) and the melting of ice caps. From 2006 to 2018, the global mean sea level has increased at rates between 3.2 and 4.7 mm/yr, which represents a faster rate than any observed in the past three millennia (IPCC 2021). Concurrently, coastal zones around the globe have been increasingly occupied and have undergone many morphological, socio-economic, and environmental changes (Neumann et al. 2015). It is estimated that one billion people currently live in coastal areas below 10 m above the high tide level, of which 230 million live below 1 m above the high tide level (Kulp and Strauss 2019). Those coastal communities and environments are therefore extremely vulnerable to coastal hazards like storms and flooding, especially in a fast-changing climate (Neumann et al. 2015). This is especially true in low-lying coastal landforms such as barrier islands (Nave and Rebêlo 2021; Nienhuis and Lorenzo-Trueba 2019). Different studies have shown that low-lying coastal areas like coastal wetlands, lagoons, and estuaries are particularly vulnerable to sea level rise due to their low elevation and their ecological and socio-economic importance (e.g., Blankespoor et al. 2014; Davies-Vollum and West 2015; Silveira et al. 2021; Al-Nasrawi et al. 2021).

The most common way to measure the potential flooding impacts induced by SLR on the world's coasts is by computing a still water level above a digital elevation model (DEM) (e.g., 1 m higher than the current shoreline) (Ferreira et al. 2021). This method is called a "bathtub approach" (Poulter and Halpin 2008). Yet, this approach maximizes inundation (Poulter and Halpin 2008; Williams and Lück-Vogel 2020; Lopes et al. 2022) mainly because it

✉ Raphaelle Croteau
raphaelle.croteau@hotmail.com

André Pacheco
ampacheco@ualg.pt

Óscar Ferreira
oferreir@ualg.pt

[1] CIMA/ARNET, Universidade do Algarve, Campus de Gambelas, 8005-139 Faro, Portugal

does not include the future land elevation variation, which can be induced by marsh growth or coastal erosion (Poulter and Halpin 2008), does not consider the infiltration of the water in the sand or the surface roughness (Poulter and Halpin 2008; Li et al. 2014; Williams and Lück-Vogel 2020; Lopes et al. 2022), and assumes a long-lasting water level (Li et al. 2014). As a result, several authors have attempted to develop methodologies to improve the simple bathtub approach (e.g., Li et al. 2014; Williams and Lück-Vogel 2020; Terres de Lima et al. 2021). One of the main challenges in modelling coastal inundations is that different systems will have different environmental responses toward coastal flooding (e.g., open ocean coast vs. backbarrier estuary). Due to the high variability of the world's coastal geomorphology, SLR impacts can only be evaluated precisely at local scales (Cazenave and Cozannet 2014) and different types of coastal floods (e.g., storm surge related flood, SLR related inundation, and wave related flood) cannot be modeled equally.

In addition to the flooding hazard, coasts of the world are greatly affected by human influences, such as coastal urbanization (Halpern et al. 2007; Elliott et al. 2019), pollution (Halpern et al. 2007; Defeo et al. 2009), disruption of natural sediment regimes (Hsu et al. 2007; Defeo et al. 2009; Carrasco et al. 2012; Kombiadou et al. 2019), destruction of coastal environments (e.g., mangroves and marshes) (Halpern et al. 2007; Elliott et al. 2019), and infrastructure construction (Halpern et al. 2007; Hsu et al. 2007; El-Asmar et al. 2016; Kombiadou et al. 2019; Sakhaee and Khalili 2021). These disruptions of the natural coastal environment have numerous impacts, especially on sandy coasts (Yincan 2017). More specifically, the construction of ports and harbors is known to significantly influence the hydrodynamics, sediment regimes, and ecosystems of coastal environments (El-Asmar et al. 2016; Shenghui et al. 2018; Barbaro et al. 2019). The most common morphological impacts induced by the construction of harbors are erosion, scour, and sedimentation (Sakhaee and Khalili 2021). Various case studies on the topic have been published recently about open ocean and sea environments (e.g., Song et al. 2017; Barbaro et al. 2019; Duarte et al. 2018; Shenghui et al. 2018; Ghaderi and Rahbani 2020; Sakhaee and Khalili 2021), estuaries (e.g. El-Asmar et al. 2016; Prumm and Iglesias 2016), and lakes (e.g. Mattheus and Diggins 2019), but very few have discussed the morphological impacts of harbor construction in backbarrier environments.

Understanding how the increase in total water level (TWL) combined with anthropized shorelines will impact coastal occupation is necessary to maintain the safety of the communities and infrastructures. Thus, this study intended to compare the shoreline evolution of a small village in the South of Portugal (Culatra) before and after the construction of a harbor and associated beach nourishment and includes both the SLR and post-construction shoreline evolution trends within a coastal flooding analysis. The specific objectives of this study were to: (1) define the morphological evolution of Culatra's backbarrier shoreline before and after the construction of the harbor and the beach nourishment; (2) assess the vulnerability of the village to inundation by extreme TWL based on scenarios of SLR and shoreline retreat; (3) propose coastal management measures based on the observed coastline's evolution and the potential flooding for 2050 and 2100.

Study area

The study area is the village of Culatra and the surrounding coastline located on the center of the backbarrier of Culatra Island, one of the five islands of the Ria Formosa barrier island system in the South of Portugal (Fig. 1). The Ria Formosa Natural Park includes the biggest coastal lagoon environment in Portugal with an area of 84 km^2 (Andrade 1990). It extends for approximately 55 km in the W-E direction and between ~ 0.5 and 8 km in the N-S direction. The islands' topography is dominated by vegetated dunes with a continuous frontal dune of *c.* 5 to 10 m high on the oceanside (Pilkey et al. 1989). The lagoon side was formed by the accumulation of fine sands, and its colonization by halophile vegetation created large sand tidal flats and salt marshes (Pilkey et al. 1989). Today, these tidal flats and salt marshes represent two thirds of the whole lagoon area (Carrasco et al. 2021) and the lagoon has an average depth of less than 2 m below mean sea level (Andrade 1990).

Culatra Island is approximately 7.45 km long and has an average width of ~ 480 m in the eastern part of the island while it is ~ 390 m on the western side (Garcia et al. 2010). Culatra village is the largest and the only one with permanent occupation on the island (Fig. 2A) with a population of about 1000 people, although it triples during the summer (May to September) due to tourism (Pacheco et al. 2021). The main economic activities are related to fishing and mollusc farming, and tourism (Pacheco et al. 2021). The vast majority of the buildings on the island are residential homes with some commercial and municipal infrastructures (Carrasco et al. 2013). Many of those infrastructures are located less than 100 m from the sea, putting them potentially at risk to inundation (Carrasco et al. 2013).

The morphology of Culatra Island, its coastline, and backbarrier shoreline have been highly altered by the opening and stabilization of the Faro-Olhão Inlet between 1929 and 1955, and the different engineering works that took place until 1955, and in the 1980s (Pacheco et al. 2011).

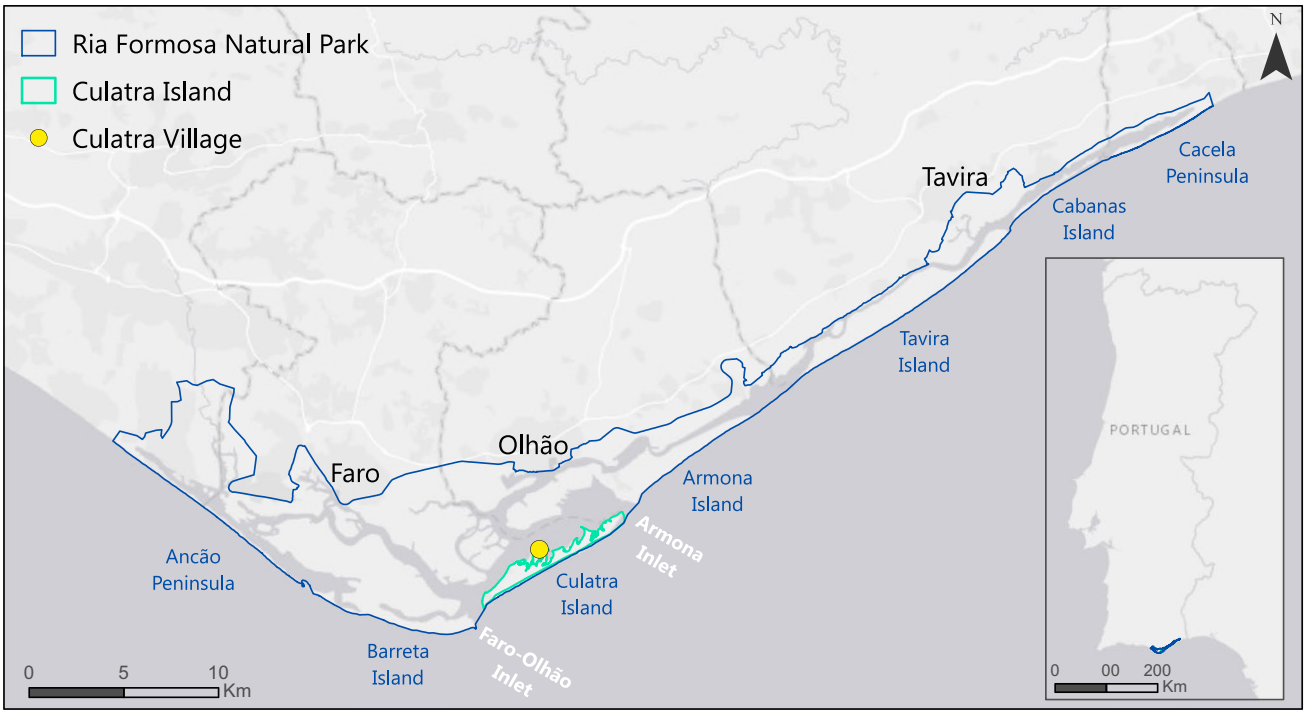

Fig. 1 Location of Culatra Island and village within the Ria Formosa in southern Portugal

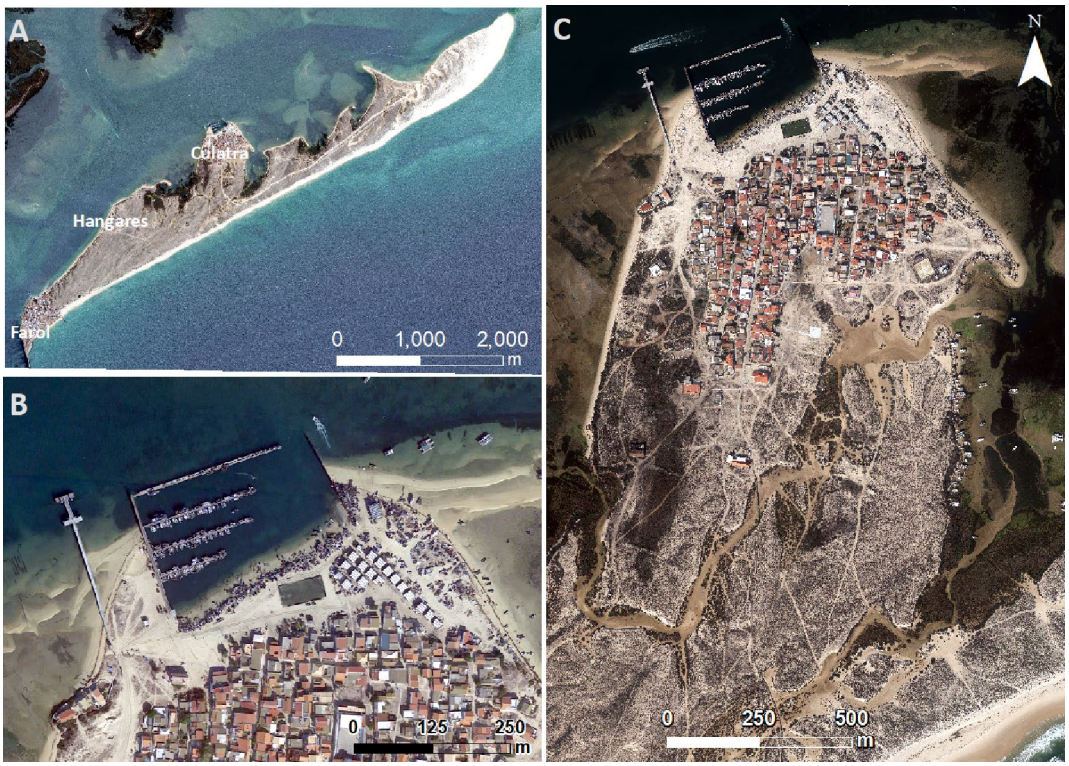

Fig. 2 (**A**) Culatra Island and its three villages: Farol, Hangares, and Culatra; (**B**) Detailed view of the built harbor in Culatra village and the nourishment that took place in the vicinity of the harbor to avoid the periodical inundation of the buildings; (**C**) Culatra village. Images from Google Earth

The most notable morphological change is the elongation of the island to the East by ~ 3000 m between *c.* 1950 and 2015 (Garcia et al. 2010; Kombiadou et al. 2018, 2019; Nave and Rebêlo 2021). The opening and stabilization of the Faro-Olhão Inlet also impacted the backbarrier of Culatra Island resulting in the overall eastern extension of Culatra's backbarrier by 38% when comparing the area from 1952 with the one from 2014 (Kombiadou et al. 2019). Localized erosive areas might be related to anthropogenic pressures such as navigation and shellfish harvesting (Kombiadou et al. 2018).

Culatra village is rather sheltered from the most energetic ocean related storm impacts. Because the fetch is very limited in the lagoon (maximum ~ 6 km in Culatra), it does not allow the formation of high and long waves (Carrasco et al. 2011). Tides are the major sediment transport mechanism within the Ria Formosa (Salles et al. 2005). The tidal regime is semidiurnal mesotidal and the typical average tidal range is 2.8 m for spring tides, with a maximum range of 3.5 m, and 1.3 m for neap tides (Pacheco et al. 2008, 2011; Carrasco et al. 2009; Ferreira et al. 2016). Storm surge can be relevant, with average heights of about 0.36 m at the Huelva Tide Gauge in Spain (Almeida et al. 2012), located ~ 80 km from the Ria Formosa, and maximum heights in the order of 0.6 m (Ferreira et al 2019).

In the past, several flooding events caused damages to residences and other infrastructures (Carrasco et al. 2013). Preventing the consequences of such events was one of the motivations for the construction of the harbor and the nourishment of the surrounding beaches between 2007 and 2011 (Fig. 2B, C). This fishers' harbor was also built to provide a space for fishers to park their boats in safe conditions and to protect the cultural and natural heritage of the Ria Formosa as the ~ 100 boats previously needed to anchor which was damaging the lagoon bed and its ecosystem (Hidroprojecto 2005). The associated beach nourishments consisted in elevating the shores on both sides of the harbor to 4.5 m higher than the mean sea level and regulating the beach with a slope inclination of 1:4.

As for the SLR, localized projections have been developed by Fox-Kemper et al. (2021) and Garner et al. (2021a, b) based on the different shared socio-economic pathways (SSP) presented in the report from the international panel on climate change (IPCC 2021). For the Algarve, the closest projections available are in Lagos, approximately 80 km to the east of the study area. The median likely confidence level rates of SLR are predicted to be 6.8 mm/yr (SSP 3–7.0), 7.3 mm/yr (SSP 5–8.5), and 7.8 mm/yr (low confidence SSP 5–8.5) between 2040 and 2060 and 10.1 mm/yr (SSP 3–7.0), 12.1 mm/yr (SSP 5–8.5), and 16.0 mm/yr (low confidence SSP 5–8.5) between 2080 and 2100 (Fox-Kemper et al. 2021; Garner et al. 2021a, b).

Methodology

Shoreline evolution

The backbarrier shorelines were extracted from a set of eight images covering the 1996–2021 period (26 years). The set included two historical aerial photos (1996 and 1999) and two orthophotographs (2002 and 2014) that were provided by the Centro de Informação Geospacial do Exército (CIGeoE) and the Direção Geral do Território (DGT). To increase the temporal resolution of the analyzed period, Google Earth images were used to complete the period up to 2021. The Google Earth images were downloaded in high quality (pixel density of 4800 × 3047) for the years of 2007, 2011, 2017, and 2021. The downloading process was done at an eye altitude of 613 m while ensuring no image tilting. Three images per year covering the study area were downloaded to increase the image quality, one for the northern part of the village (e.g., 2007_1), one for the southern part of the village (e.g., 2007_2), and one for the coastline adjacent to the village on the East (e.g., 2007_3) (Table 1). To improve the quality of the georeferencing of the aerial images and orthophoto, they were separated into two sections, one for the West and another one for the East side of the study area. The georeferenced orthophoto from 2014 projected in

Table 1 X, Y, and total root mean square error (RMSE) for each georeferenced image. For the Google Earth images, 20XX_1 corresponds to the northwest image, 20XX_2 corresponds to the southwest image, and 20XX_3 corresponds to the eastern image. For the aerial photos and orthophotos, W corresponds to the village area while the E corresponds to the coastline adjacent to the east of the village

	Image	X RMSE (m)	Y RMSE (m)	Total RMSE (m)
Google Earth images	2007_1	0.105	0.025	0.108
	2007_2	0.303	0.185	0.355
	2007_3	0.106	0.017	0.108
	2011_1	0.268	0.105	0.287
	2011_2	0.251	0.086	0.266
	2011_3	0.288	0.118	0.311
	2017_1	0.142	0.033	0.146
	2017_2	0.152	0.038	0.157
	2017_3	0.279	0.172	0.328
	2021_1	0.263	0.103	0.283
	2021_2	0.100	0.012	0.101
	2021_3	0.137	0.022	0.139
Aerial photos and orthophoto	1996_W	0.325	0.150	0.357
	1996_E	0.327	0.215	0.392
	1999_W	0.275	0.125	0.302
	1999_E	0.173	0.050	0.180
	2002_W	0.212	0.068	0.223
	2002_E	0.128	0.021	0.129

ETRS 1989 Portugal TM06 was used as the base image for the georeferencing of the rest of the images due to its high resolution (pixel size of 0.01 m). All the images were georeferenced using four to six reference points with the georeferencing tool from ArcMap 10.8 (ESRI 2019). To ensure the accuracy of the georeferencing process, the root mean square error (RMSE) was calculated for each image. Ten control points were drawn sparsely across each image in different locations than the points used for the georeferencing. Then, the coordinates from the predicted (georeferenced image) and correct (referenced 2014 orthophoto) control points were extracted to calculate the RMSE. The residuals squared for each point were calculated by subtracting the predicted coordinates from the correct ones in X and Y and squaring the results. The RMSE in X and Y was calculated using Eq. 1:

$$RMSE\ in\ X\ or\ Y = \frac{\sqrt{\sum(squared\ residuals\ in\ X\ or\ Y)}}{number\ of\ control\ points} \quad (1)$$

The total RMSE was then calculated using Eq. 2:

$$Total\ RMSE = \sqrt{(X\ residuals)^2 + (Y\ residuals)^2} \quad (2)$$

The total RMSE for the Google Earth images and aerial photos (Table 1) were all below 0.4 m and on average around 0.25 m which was considered acceptable for the intended analysis.

For most areas, except in the vicinity of the harbor and the coast adjacent to the East of the harbor, the edge of the stable vegetation (the transition line between the beach sand and the bushy and rugose vegetation) was chosen as the proxy for the backbarrier shoreline (Fig. 3A), as was done by Kombiadou et al. (2019). In the absence of such vegetation (e.g., due to coastal occupation), the dune scarp was used as the shoreline proxy, when present (Fig. 3B). Finally, where none of the previous features was present, the highest water level was used, identified by the inward line formed by the accumulation of zoostera or debris (Fig. 3C). The shorelines were also divided into two different groups, the regular shorelines, and the artificially stabilized shorelines. The artificially stabilized shorelines were excluded from the calculations of the shoreline evolution.

The digital shoreline analysis system (DSAS) version 5.1 (Himmelstoss et al. 2018) was used to compute the shoreline evolution before (1996 to 2007) and after (2011 to 2021) the harbor's implementation and the associated beach nourishment. First, a baseline was drawn offshore from the different shorelines before and after the harbor construction. Then, transects were placed every 15 m perpendicular to the baseline while covering all the shorelines. The uncertainties used for the DSAS computations are the ones from

Fig. 3 Examples of the features used to delineate the shorelines. **A**) Stable vegetation. **B**) Dune scarp, when no stable vegetation was present. **C**) Maximum high-water level when no stable vegetation or dune scarp were present

the georeferencing (Table 1). The uncertainty related to the shoreline mapping was minimized because the shorelines were mostly extracted at the same zoom level and by the same operator. The weighted linear regression (WLR) was used as it is the most statistically robust from the DSAS analysis because it emphasizes on the data with lower uncertainties (Himmelstoss et al. 2018). The shoreline displacement was considered stable when the observed variation was smaller than 0.4 m/year (which represents the maximum RMSE calculated), a small erosion/accretion between this value and its double, and strong erosion/accretion when above 0.8 m/yr. Negative values indicate erosion while positive ones indicate accumulation (Table 2). The pre-harbor observed trends were grouped into thirteen sectors according to their similarities to facilitate the analysis (e.g., similar erosive transects within the same area were grouped in a sector). The same sectors were also used to analyze the post-harbor trends.

Flooding cartography

To determine the inundation hazard, a new flood mapping methodology was elaborated based on the definition of the total flood extension and presents an alternative to the widely used simple bathtub approach. A LiDAR DEM was used as the elevation proxy of the area. It was obtained from the Direção-Geral do Território (DGT) and has a precision of 2 m horizontally and < 30 cm vertically (Sistema Nacional de Informação Geográfica 2011). The relevant files representing the study area were merged and projected in ETRS 1989 Portugal TM06.

The TWL (tide + surge + SLR) was used to compute and map the potentially flooded areas according to different SLR scenarios. The predicted SLR values used were based on the latest IPCC report for Lagos, Portugal (Fox-Kemper et al. 2021; Garner et al. 2021a, b). The average SSP 5–8.5 was used because it is the scenario that will be observed at a global scale if the greenhouse gas emissions are not drastically reduced in the coming decades (IPCC 2021), and is the most widely used for future climate change impact simulations. The storm surge and maximum high tide levels were adapted from Carrasco et al. (2012) (Table 3).

Table 2 Classification of the trends obtained with the weighted linear regression (WLR) rates and the color code associated with each class

Classification	WLR (m/yr)	Color Code
Strong Retreat	≤ -0.8	
Small Retreat	]-0.8; -0.4[	
Stable	[-0.4; 0.4]	
Small Accretion	]0.4; 0.8[	
Strong Accretion	≥ 0.8	

Table 3 Total water levels used in this study based on the tides and storm surge levels computed by Carrasco et al. (2012). The return periods are for the tides + surge levels. The total water levels are presented for the current scenario and the median *likely* SSP 5–8.5 scenario (Fox-Kemper et al. 2021; Garner et al. 2021a, b) in Lagos, Portugal for two years of reference: 2050, and 2100

	Total Water Level (m)		
Return Period (years)	Current	2050	2100
1	2.02	2.28	2.82
100	2.48	2.74	3.28

First, the simple bathtub approach (Poulter and Halpin 2008) of each flooding scenario was applied on the DEM to determine the potentially flooded areas. The pixels with higher altitudes than the ones for each level were reclassified as "not a number" (NaN), i.e., they would not be flooded even when using the simple bathtub approach. Based on the reclassified values for each scenario, a cost distance analysis was performed in ArcMap as the first step to define the flood extension. The dune crest (highest elevation near the beach/dune contact) was used as the origin for the distance computation (flooding source). The water depth (h_c) was calculated with the Raster Calculator by subtracting the elevation of each pixel from the flood level for each scenario. The Raster Calculator was also used to compute the flooding velocity (u_c) according to the expression developed by Donnelly (2008) for overwash in sandy beaches:

$$u_c = 1.53\sqrt{g h_c} \tag{3}$$

where g is the acceleration of gravity. u_c was considered as a proxy for the flood extension in the absence of an equation specifically developed for tide + surge + SLR.

Finally, the Raster Calculator was used to apply the expression from Plomaritis et al. (2018) that defines the potential flooding extension:

$$h(x) = h_c \exp\left(-a\frac{x}{u_c}\right) \tag{4}$$

where $h(x)$ represents the water elevation at a distance x from the flooding source, h_c is the water depth, a is a constant associated with the rate of infiltration of the water in the soil. In this study, the constant 0.12 was used as the infiltration value because it is a typical one for barrier islands like Culatra (Donnelly et al. 2006). x represents the distance from the flooding source, and u_c is the overwash/flooding velocity.

In addition to the six scenarios described in Table 3, two others were added to the TWL of 2050 for 1-year and 100-year return periods but this time including a projection of the shoreline retreat for 2050. The average shoreline evolution trends of the five sectors surrounding the village were computed to determine which were retreating. To do so, the

trends of the transects contained in each sector were averaged to determine a general trend for the sector. The erosive sectoral trends were included in a second flooding simulation for 2050. A new position of the dune crest was estimated for 2050 by multiplying the average sectoral trend by 29 years ((2050–2021) + 1) e.g., the average shoreline retreat for sector 5 was -0.72 m/yr, the dune crest was therefore displaced inland by 20.98 m for the second simulation. This new dune crest was used as the origin for the cost distance analysis (x value) and the overwash/flooding extension.

After computing the overwash/flooding extension, the values with an inundation value below 1 cm were considered irrelevant and were removed from the final cartography. In addition, the non-hydraulically connected polygons were removed from the cartography i.e., areas that are considered flooded by the cartography but are not connected to a flooding source (Poulter and Halpin 2008). The "four-side rule" was used, meaning that only the cells related to a flooded one through one of the four sides of the pixel were considered hydraulically connected (Poulter and Halpin 2008).

Finally, the flooded areas for each scenario were compared to the occupied areas of the village. A shapefile was created with the different occupied areas (buildings, main walking paths, football field, helipad, etc.) and was intersected with the flooded areas to determine the part of the occupied zones that would be flooded according to the TWL scenarios.

Results

Shoreline evolution

The shoreline trends before the harbor construction reveal numerous stable sectors (1, 4, 7, 8, and 11) with some accretional (sectors 2, 3, 5, 9, and 13) and erosional (sectors 10, and 12) hotspots (Fig. 4A). It is also possible to observe more active tidal channels in sector 1 (breaks in the shoreline continuity) before the harbor construction. The shoreline trends after the harbor construction and beach nourishment show more extensive erosional (sectors 2, 3, 5, and 6) and accretional (sector 4) sectors around the village, but greater stability on the eastern shoreline, outside the village (sectors 8 to 13) (Fig. 4B). The harbor area and its vicinity (sectors 2, 3, and 5) show a clear shift in behavior: they were accretional before and shifted to erosional after the harbor construction. Conversely, sector 4 evolved from stable to highly accretional (Fig. 4A, B). Of the 172 pre-harbor transects evaluated, 74 were erosional (43.02%) and 98 were accretional (56.98%), while after the harbor construction, 87 transects were erosional (49.43%) and 89 were accretional (50.57%) for a total of 176 transects analyzed.

The global average WLR rates were 0.1 m/yr before and after the harbor construction. The maximum WLR erosion rates were -1.3 m/yr before the harbor construction (Figs. 4A and 5A – sector 12), and -1.6 m/yr after (Figs. 4B and 5B – sector 2). On the other end, the maximum pre-harbor accretional rate was 2.6 m/yr (Figs. 4A and 5A – sector 5), while the post-harbor one was 2.3 m/yr (Figs. 4B and 5B – sector 4).

Four sectors around Culatra village (2, 3, 5, and 6; Fig. 4B) presented erosive trends after the harbour implementation (respectively -0.44 m/yr, -0.40 m/yr, -0.25 m/yr, and -0.72 m/yr). Those four average erosive trends were projected for the year 2050. In 2050, this would represent an average shoreline retreat of -12.8 m (sector 2), -11.7 m (sector 3), -7.2 m (sector 5), and -21.0 m (sector 6). The dune crest (coastline) position was therefore moved back further inland accordingly (Fig. 6).

Flooding cartography

The flooding impacts are minimal for the current scenario with a 1-year return period and even considering the 100-year return period, but extensive for the 2100 scenario namely when considering a 100-year return period (Fig. 7). The potential flood shows a high horizontal expansion between 2050 and 2100. The flooding extension for 2050 with a return period of 100 years is very similar to the one for 2100 with a 1-year return period, indicating that what is presented as an extreme event in ~ 30 years could be very common in ~ 80 years.

The projected flooded area has always a higher extension on the West side of the harbor compared to the East one (Fig. 7). Flooding through the tidal channel in the South is minimal in all scenarios except for the 2100 ones. The shoreline retreat has minimal flooding impact compared to the increase in TWL due to SLR (Table 4). The 1-year return period flooding extension in 2050 with and without shoreline retreat would be identical (Table 4), although the 100-year return period results reveal a more extensive inundated area within the harbor (sector 3) and the eastern spit (sectors 5 and 6) (Figs. 4 and 7). The shoreline retreat by 2050 would cause and additional flooding of 3135 m^2 (for the 100-year return period) on the eastern part of sector 3 and in sector 5 compared to the results without including it (Table 4). The flooded area with a 1-year (100-year) return period will increase by 6.3 (2.3) times by 2050 and 55.9 (4.3) times by 2100 when compared to the current scenario (Table 4).

The present scenario with a 1-year return period causes minimal impact to the occupied area because it would only flood some walking paths. In 2050 with a 100-year return period, with or without shoreline retreat, the flood would reach the main village and not only affect isolated houses

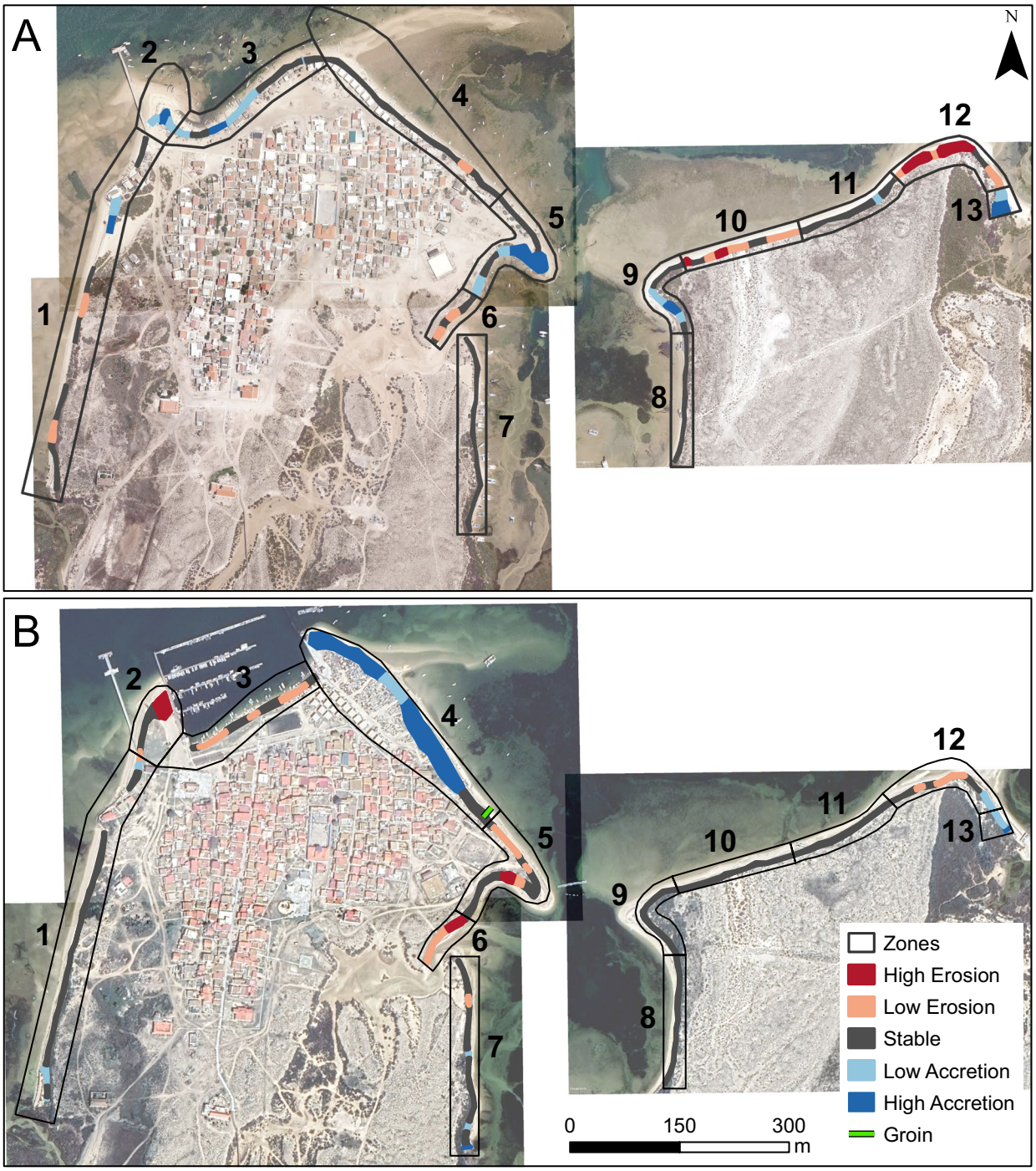

Fig. 4 (**A**) Shoreline evolution rates (m/yr) before (1996–2007); and (**B**) after (2011–2021) the harbor construction and the beach nourishment

and the football field, but also restaurants, the helipad, the community center, fishing huts, and the main walking paths (Fig. 7). The potential flooding in 2100 with a 100-year return period would impact almost 86% of the occupied area (Table 4), which includes all the main infrastructures of the village.

Discussion

Influence of the harbor construction on the shoreline evolution

The evolution of a backbarrier shoreline is usually very slow (Carrasco et al. 2011) and, overall, the results show a coastline evolving gradually, but that undeniably changed

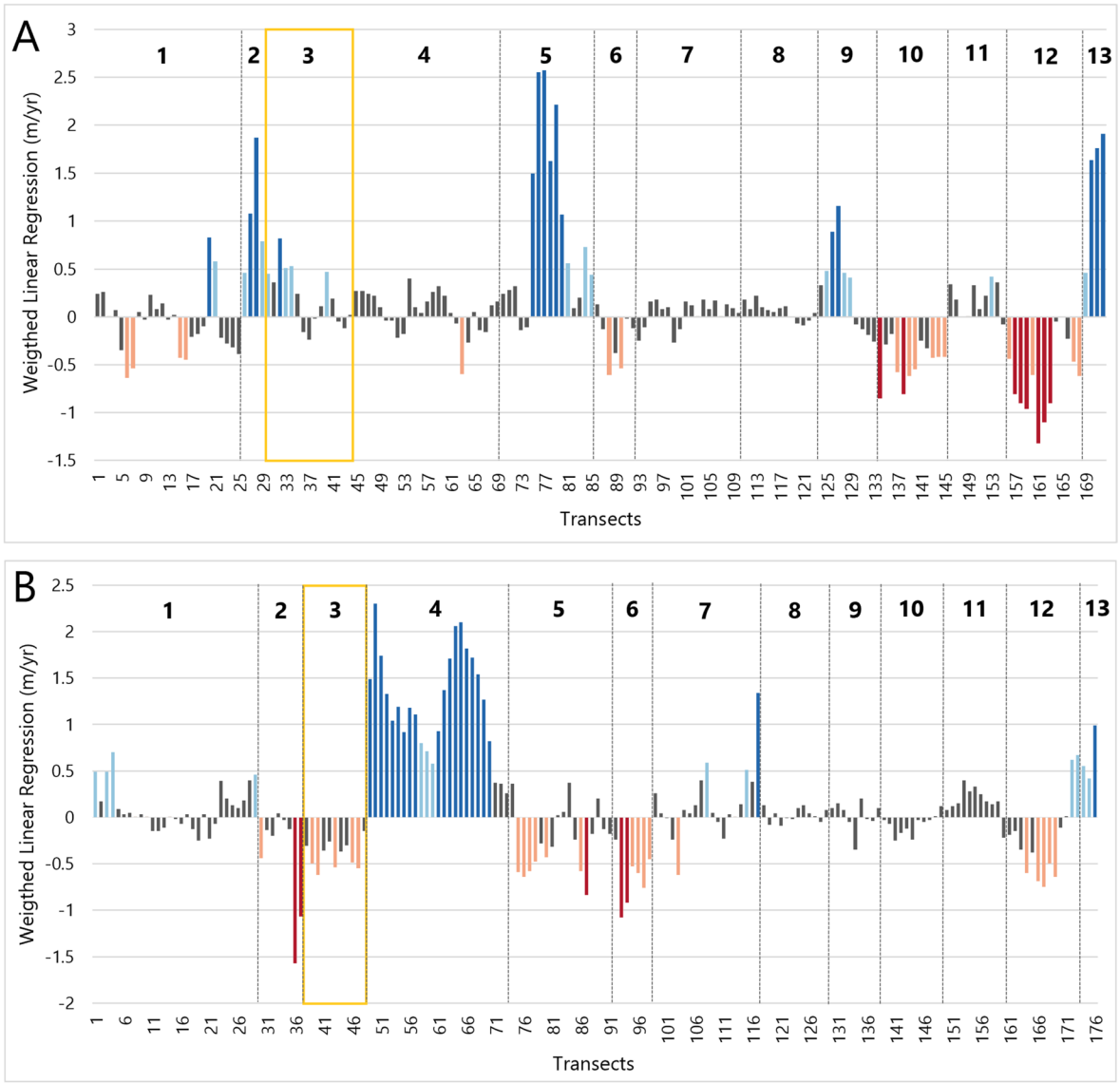

Fig. 5 Weighted linear regression rates (m/yr) for each transect analyzed (**A**) before and (**B**) after the harbor construction and the beach nourishment. The numbers above each section of the graphs represent the different sectors from Fig. 4. The yellow rectangles represent the harbor area

since the harbor construction and associated beach nourishment, especially in the vicinity of said harbor. The accretion (shoreline trends above 0.4 m/yr) observed before the harbor construction in sector 2 (Figs. 4A and 5A) was most likely caused by the accumulation of sediments transported by the dominant currents within this area of the Ria Formosa (Pacheco et al. 2008). These sediments accumulated as recurved small spits and eventually, around 2007, attached to the main shoreline. This area in the vicinity of the harbor was subject to nourishment during the construction works which altered its natural evolution. The strong erosion observed after the harbor construction and nourishment could be related to the readjustment of the slope and the overall morphology to a more natural one. Human activities such as boat launching and tractor transportation are also very important, which could promote erosion and the lowering of the area, allowing an inland displacement of the water line. In addition, this sector is affected by wakes generated by ferryboats and the boats' passages from and toward the harbor. Wakes can promote the resuspension of sediments and alter the topo-bathymetry of the backbarrier shoreline (Herbert et al. 2018).

The low erosive trends within the harbor (Figs. 4B and 5B – sector 3) could again be related to strong human activities and the readjustment of the slope following the harbor construction and the nourishment. The shoreline trends of sectors 4, 5, and 6 (Figs. 4B and 5B) are intrinsically related due to the construction of a small groin between sectors 4 and 5.

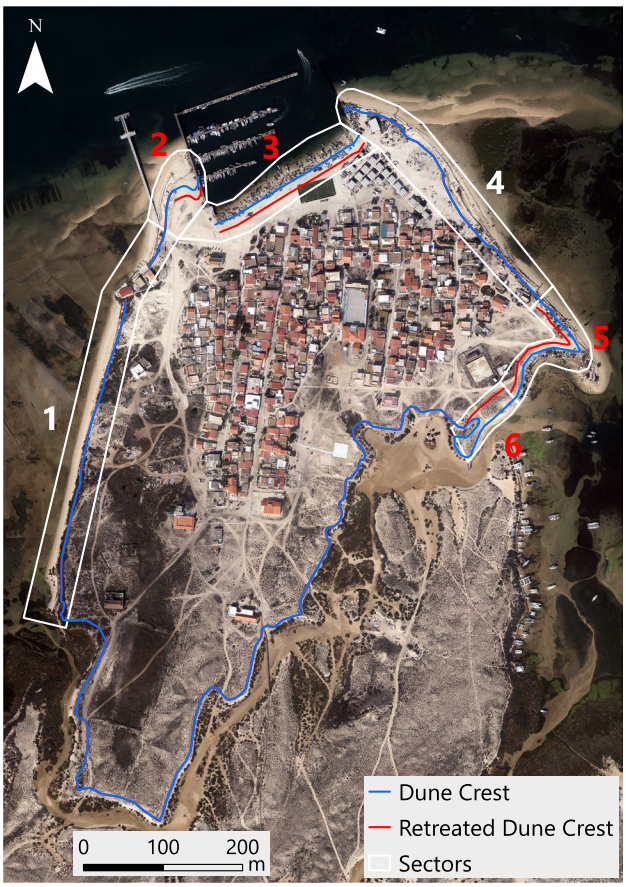

Fig. 6 Dune crests used as the proxies for the cost distance analysis. The blue line represents the current dune crest while the red ones represent the future dune crest based on the average shoreline retreat of the eroding sectors from the shoreline analysis (see Fig. 4)

Sectors 4 and 5 were previously stable and in accretion, but the combination of the construction of the harbor and the small groin disturbed their evolution. A strong accumulation then arose in sector 4 while sectors 5 and 6 were sediment deprived, indicating a dominant southwest-northeast longshore transport in the coastal sector. The construction of the groin appears to have had a greater influence on the evolution of sector 4 than the harbor did. The beach nourishment in the vicinity of the harbor could have encouraged the accumulation of sediments on the north of the groin. Finally, the erosion and accumulation seen in sectors 12 and 13 before the harbor construction decreased afterwards, indicating that this section of the shoreline is almost stable and does not show any impact from the harbor construction.

The chosen timeframe as part of this study was limited to a total of 20 years to attempt to understand the human-made perturbations caused by the harbor construction in this specific location. Therefore, the changes observed can not directly be associated with the natural long-term evolution of the island related to SLR, hydrodynamic adjustments, and salt marshes' migration. Nonetheless, it is possible to assume that the harbor construction and associated beach nourishment could have interfered with the maturing process that the backbarrier and salt marshes were going through. Indeed, Carrasco et al. (2008) observed a landward displacement of Culatra Island between 1947 and 2001, and its backbarrier was classified as immature in 2001. According to Kombiadou et al. (2019), the western part of Culatra's backbarrier (including Culatra village) was relatively stable between 1952 and 2014 and the salt marshes were classified as stable to immature during the same time period. The slow maturing process observed on the backbarrier of Culatra is mostly associated with the numerous anthropic interventions that were completed in the area within the last century, especially the opening and stabilization of the Faro-Olhão Inlet (Kombiadou et. 2018). This intervention caused a sediment imbalance between the import and export which increased the amount of sediments being trapped inside the Ria Formosa (Pacheco et al. 2008, 2011). A longer interval can therefore be expected before reaching complete marshes and backbarrier stability, especially considering the future uncertainties related to climate change (see Carrasco et al. 2021) and the other on-going human interventions such as navigation channel maintenance and harbor construction.

Potential flooding in Culatra village

The inundation results showed that the flooded occupied areas would be minimal for a 1-year return period within the current and 2050 scenarios. However, the village would be greatly impacted by an inundation occasioned by a 100-year return period. This indicates that the village is somewhat protected for the near future recurrent TWL but will require some adaptations to prepare against future major TWL since the flooded occupied areas increase drastically for the 2050 and 2100 scenarios with a 100-year return period (Table 4).

The obtained results agree with the field observations during the Emma Storm in 2018 (TWL return period of 6–7 years) (Ferreira et al. 2019) when no flooding was observed within the main village. They seem to disagree with Lopes et al. (2022) who state that the backbarrier of Culatra would be almost completely flooded between 2046 and 2065 with a 2-year return period. They also disagree with the results from Carrasco et al. (2013), Antunes (2019) and Antunes et al. (2019) (see https://arcg.is/0u5XnL) which suggest that Culatra Island would be highly flooded by 2050. These last studies consider the areas as impermeable and the TWL as a permanent inundation level that affects the entire area regardless of their position or hydraulic connectivity. Thus, they maximize the flooded area to a level that is not consistent with reality. This study provides a more precise flood mapping of Culatra village compared to the studies mentioned above because it was performed at a

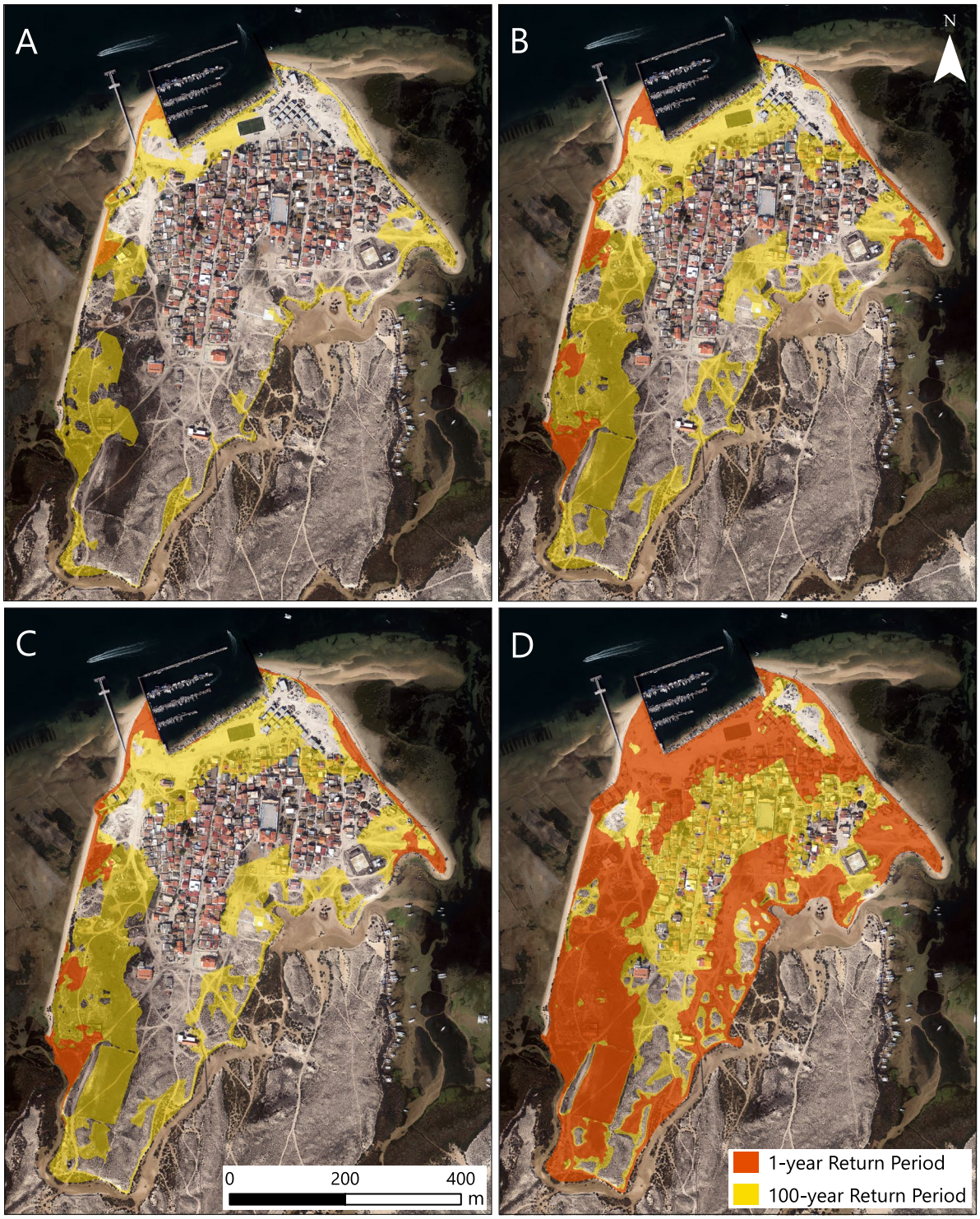

Fig. 7 Flooding cartography for return periods of 1 year (orange) and 100 years (yellow). (**A**) Current scenario; (**B**) 2050 scenario; (**C**) 2050 scenario including the average shoreline retreat rates projected in 2050 for sectors 2, 3, 5, and 6 (see Figs. 4B, 5B);)D) 2100 scenario

higher resolution and, more importantly, because the developed methodology considers water infiltration and dune crest retreat. This is relevant considering that presenting exaggerated results to the public can have counterproductive effects by discrediting the relevance of climate change science (Lopes et al. 2022).

Table 4 Flooded areas according to the different total water level scenarios considered, the flooded occupied areas, and the proportion they represent compared to the occupied area. Total analyzed and occupied areas (bottom line)

Scenario	Flooded Area (m^2)	Flooded Occupied Area (m^2)	Flooded Occupied Area (%)
Current 1-yr RP	2 837	153	0.13
Current 100-yr RP	59 761	5 488	4.60
2050 1-yr RP	17 841	1 454	1.22
2050 100-yr RP	136 741	27 545	23.11
2050 1-yr RP (Retreat)	17 841	1 454	1.22
2050 100-yr RP (Retreat)	139 876	30 365	25.47
2100 1-yr RP	158 689	39 437	33.08
2100 100-yr RP	254 160	102 216	85.75
Total	294 632	119 202	

The scenarios used as part of this study and the ones from the studies presented above did not include morphodynamic feedback induced by flood events, i.e., the readjustment of the dune crest or the dune area due to higher water levels. The increased flooding frequency and intensity would promote dune lowering and eventually dune loss, which represents a positive morphodynamic feedback that could lead to more flooding events. This kind of feedback could be especially problematic in locations where sedimentation rates are lower than SLR, which would occasion strong coastal retreats (Zhou et al. 2022). The assessment of such feedback would require more complex modelling, hence their exclusion from this study.

One of the most important factors when modelling the potential inundation hazard is the TWL used. Despite the fact that the SLR projections developed by IPCC (2021) are the most accurate and recent ones in the literature at the moment, they still contain uncertainties – mostly related to future greenhouse gas emissions – that could considerably alter the SLR projections. The median value for the high confidence scenario (SSP 5–8.5) was considered representative of future conditions but a wide range of scenarios could be tested with different results. The projections of TWL used in this study also assume that the past storm surge and tidal levels will remain the same over the next century. However, Vousdoukas et al. (2016) showed that storm surge levels along the southern Portuguese coast could slightly decrease within this century, which would also slightly decrease the TWL and therefore the extension of inundations. Pickering et al. (2017) studied the impacts of SLR on tidal levels and showed that when increasing the global water level by 2 m, the mean high-water level could increase by 0.05 m when considering coastal retreat or on the opposite decrease by 0.02 m when considering a fixed present-day coastline. A further increase in water level could facilitate the propagation of long waves (e.g., tidal waves) inside the lagoon by reducing bottom friction which, in turn, would increase the inundation levels, the opposite is also true (Lopes et al. 2022). This could be an important factor for the west side of the village, which is the most impacted among the scenarios, but is also the area where the vegetation is highest and most stable. The presence of stable vegetation in this area could increase bottom friction and decrease the flooding velocity and extension. On the contrary, the presence of several impermeable concrete walking paths within the island would prevent the infiltration of the water and accelerate the tidal wave propagation further inland. The expansion of the flood would increase the risk to the occupied area including places with higher social and economical value (e.g., community center, restaurants, and helipad).

Another important factor for inundation mapping is the quality of the elevation model used (Poulter and Halpin 2008). In this case, the DEM used has a good horizontal and vertical resolution, but it is relatively old (2011) considering that the shoreline has evolved since and that other beach nourishments and terrain modifications have taken place in the last 11 years. The elevation model also contained some errors regarding the elimination of the elevated features such as buildings (some areas showed elevations above 4 m shaped as perfect squares). It was however considered to be representative of the vast majority of the area in its present condition because the dune morphology is stable and only a relatively small portion of the area was anthropically altered.

The main limitation of the methodology developed as part of this study is that the formula used was developed for overwash i.e., temporary floods caused by waves, while it was used here to determine a higher duration inundation (during high tide) and thus the obtained velocities are most likely exaggerated. However, the time over which the flood occurs (hours instead of seconds) allows continuity of the flow and probably counterbalances that exaggeration. In addition, to better assess the natural evolution of the backbarrier's response to SLR, a longer period could be analyzed.

Apart from those limitations, this new methodology includes several advantages that make it a good option to map inundations in sandy backbarrier coasts. Firstly, the slope is considered within the computations of the water propagation inland by computing the elevation relative to the

water level for each pixel. This factor was also considered in other methodologies (e.g., Sekovski et al. 2015; Didier et al. 2019; Perini et al. 2016; Williams and Lück-Vogel 2020; Terres de Lima et al. 2021). Secondly, the use of the cost distance analysis (also used by Li et al. 2014; Sekovski et al. 2015; Perini et al. 2016; Williams and Lück-Vogel 2020) allows a more accurate assessment of the possibility of propagation of the water inland compared to the simple bathtub approach. One of the improvements regarding the cost distance tool used in this study is that the analysis was repeated to determine the potential flooding impacts related to coastal erosion to provide a more complete estimation of the flooding potential in the area, including the potential shoreline evolution by 2050. The additional analysis provided more information on the importance of shoreline retreat in the coastal flooding of Culatra village and proved that the inundation mostly depends on SLR and TWL increases rather than coastal erosion. The main improvement of this methodology compared to most of the ones presented above is that it includes the infiltration of the water in the soil which can be an important decreasing water level factor in sandy substrates like barrier islands.

Coastal management measures to mitigate the impacts of coastal flooding and erosion

In the last few decades, the use of soft stabilization (e.g., beach nourishment, vegetation, restoration of wetlands, dune creation, etc.) has become a more popular approach compared to the use of hard stabilization (e.g., groin, jetty, breakwater, revetment, etc.) (Ceia et al. 2010; Bilkovic et al. 2016; Sharma et al. 2016; Waltham et al. 2021). These "soft-engineering" measures typically have lower environmental impacts, which makes them better candidates for fragile and environmentally protected systems like the Ria Formosa (Ceia et al. 2010).

Different measures can be considered to allow the community to remain in Culatra village without being exposed to a high level of hazard, which can serve as examples for other occupied areas located on backbarriers. For the current scenario and the 2050 one with a 1-year return period, no protection measures are necessary because the occupied areas that could be flooded are mostly walking paths that would only require to be cleaned after the storm or extreme water level. For the current and 2050 scenarios with return periods of 100 years, several measures should be considered to protect the community. As an example, on the West of the harbor (Figs. 4 and 5, sector 2) where erosion has been the highest of the study area since the harbor construction, anthropic disturbance (i.e. transport with tractors) should be limited. This reduction of anthropic disturbance should be coupled with the restoration of native plants. According to Feagin et al. (2009), coastal vegetation is a great way to modify and control the sedimentary dynamics of an area in response to slow events like tidal forces or SLR. Further nourishing the area without a reduction of human disruptions would lead to the same results in ten years without solving the problem in the long term. Similarly, human actions on the shoreline within the harbor should be avoided to protect it and allow vegetation to grow and create a buffer between the waterline and the village. Another example is the tidal channel on the South of the village. The vegetation there is already well implemented and not too disturbed, therefore elevating the dunes could be a good option to further protect this area from flooding. This method could prevent the inundation of several features such as the helipad, a playground, a kindergarten, and houses.

For the 2100 scenarios, the viability of the village itself is threatened by floods that would affect all the main infrastructures and many houses on a yearly basis. In such case, simple measures like the ones mentioned above (e.g., dune elevation, nourishment, and plant restoration) would most likely not be enough to protect the village and its population. Thus, three main solutions can be considered i.e.: (1) to use hard protection all around the village, for instance by building concrete walls or dikes, although this solution would highly decrease the quality of life of the habitants, would be very expensive and not acceptable within a natural park. In addition to the hard protection, some parts of the village might need to be rebuilt on elevated and stabilized ground, which would further increase the cost of this option; (2) to relocate the community. However, studies have shown that many people living in coastal communities will remain in place and accept to live at risk because they are emotionally attached to the location, the environment, their community, or for the proximity to their workplace and/or public facilities (Costas et al. 2015; Buchori et al. 2018); (3) to adapt. This solution should include a sensibilization program to present the hydro-meteorological hazards and their potential risks to the population for different scenarios and timeframes. For individual house owners, apart from relocation, long-term solutions could be to elevate the houses above a potential water level or to use an amphibious architecture (see English et al. 2016), solutions that are already used in many locations worldwide (see English et al. 2016; Liao et al. 2016; Proverbs and Lamond 2017; Buchori et al. 2018). Typically, building a flood resistant or amphibious house will increase its cost by 5 to 10% compared to a normal house (English et al. 2016). Public authorities should ensure that all new constructions are water resistant or resilient to guarantee the safety of the people and attenuate future economic, social, and health disasters. In addition, setbacks should be required and enforced by the authorities for any new construction or replacement buildings. Other less expensive adaptation solutions could be to redesign houses according to potential floods, for instance by adding high storage space, raising electrical sockets and panels, moving furniture ahead of a storm, etc. (Proverbs and Lamond 2017). For the

community to remain safe and prepare their houses for storm related floods, an early warning system and an evacuation plan should be put in place by the authorities and practiced with the community. The relocation of community could also be discussed as a potential solution. However, that would imply huge cultural, societal, and economic consequences because some of the Ria Formosa communities have a high level of place attachment and have refused to be relocated in the past (Domingues et al. 2021).

Conclusions

This study developed a method to estimate the potential ocean-driven inundation based on total water levels in a back-barrier environment and applied it to the village of Culatra (southern Portugal). The methodology also allowed assessment of the impacts of a harbor implementation on inundation patterns. The shoreline evolution was measured for a period of ~ 10 years before and after the harbor construction, aiming to understand the influence of this artificial structure on the recent coastal evolution. The sectors showing shoreline retreat between those two periods were included in the flood analysis. The flood analysis was performed using a new GIS based methodology to define the inundation extension using total water levels (tides + storm surge + sea level rise).

The results showed that the shoreline changes occurred mostly around the harbor while the rest of the study area remained relatively stable. The shoreline retreat induced by the harbor construction appeared to have a lower impact on the flooding extension in the area than the increase in water level. Due to sea level rise, the occupied flood-prone areas with a 1-year (100-year) return period of total water level could increase by 1.2% (23.1%) by 2050 and 33.1% (85.8%) by 2100, which would severely increase the risk potential in Culatra village. For the next 30 years (~ 2050), relatively easy measures can be taken to avoid important flood related damages such as elevating dunes and nourishing flood-prone areas. However, the 2100 scenarios showed that the village would require major planning, a reduction of the developed area, and architectural improvements in order for the community to remain safe.

Acknowledgements The authors acknowledge Lara Talavera for helping with the shoreline extraction. This study had the support of national funds through Fundação para a Ciência e Tecnologia (FCT), under the project LA/P/0069/2020 granted to the Associate Laboratory ARNET and UID/00350/2020 CIMA.

Funding Open access funding provided by FCT|FCCN (b-on).

Data Availability Data sets generated during this study are available from the corresponding author on upon request.

References

Almeida LP, Vousdoukas MV, Ferreira Ó, Rodrigues BA, Matias A (2012) Thresholds for storm impacts on an exposed sandy coastal area in Southern Portugal. Geomorphology 143–144:3–12. https://doi.org/10.1016/j.geomorph.2011.04.047

Al-Nasrawi AKM, Kadhim AA, Shortridge AM, Jones BG (2021) Accounting for DEM error in sea level rise assessment within riverine regions; case study from the Shatt Al-Arab River Region. Environments 8(5):46. https://doi.org/10.3390/environments8050046

Andrade CA (1990) O Ambiante de Barreira da Ria Formosa, Algarve, Portugal [Ph.D Thesis]. Universidade de Lisboa

Antunes C (2019) Assessment of Sea Level Rise at West Coast of Portugal Mainland and Its Projection for the 21st Century. J Mar Sci Eng 7(3):61. https://doi.org/10.3390/jmse7030061

Antunes C, Rocha C, Catita C (2019) Coastal flood assessment due to sea level rise and extreme storm events: a case study of the Atlantic Coast of Portugal's Mainland. Geosciences 9(5):239. https://doi.org/10.3390/geosciences9050239

Barbaro G, Foti G, Miduri M, Puntorieri P (2019) Shoreline changes caused by Marina of Badolato (Italy). International Journal of Civil Engineering and Technology 10(7):298–307

Bilkovic DM, Mitchell M, Mason P, Duhring K (2016) The role of living shorelines as estuarine habitat conservation strategies. Coast Manag 44(3):161–174. https://doi.org/10.1080/08920753.2016.1160201

Blankespoor B, Dasgupta S, Laplante B (2014) Sea-Level Rise and Coastal Wetlands. Ambio 43(8):996–1005. https://doi.org/10.1007/s13280-014-0500-4

Buchori I, Pramitasari A, Sugiri A, Maryono M, Basuki Y, Sejati AW (2018) Adaptation to coastal flooding and inundation: mitigations and migration pattern in Semarang City, Indonesia. Ocean Coast Manag 163:445–455. https://doi.org/10.1016/j.ocecoaman.2018.07.017

Carrasco AR, Ferreira Ó, Davidson M, Matias A, Dias JA (2008) An evolutionary categorisation model for backbarrier environments. Mar Geol 251(3–4):156–166. https://doi.org/10.1016/j.margeo.2008.02.009

Carrasco AR, Ferreira Ó, Freire P, Dias JA (2009) Morphological Changes in a Low-Energy Backbarrier. J Coastal Res 1:173–177

Carrasco AR, Ferreira Ó, Matias A, Pacheco A, Freire P (2011) Short-Term Sediment Transport at a Backbarrier Beach. J Coastal Res 277:1076–1084. https://doi.org/10.2112/JCOASTRES-D-09-00163.1

Carrasco AR, Ferreira Ó, Matias A, Freire P (2012) Natural and Human-induced Coastal Dynamics at a Back-Barrier Beach. Geomorphology 159–160:30–36. https://doi.org/10.1016/j.geomorph.2012.03.001

Carrasco AR, Ferreira Ó, Matias A (2013) Managing Flood Risk in Fetch-Limited Environments. J Coastal Res 65:892–897. https://doi.org/10.2112/SI65-151.1

Carrasco AR, Kombiadou K, Amado M, Matias A (2021) Past and future marsh adaptation: Lessons learned from the Ria Formosa

lagoon. Science of the Total Environment 790:148082. https://doi.org/10.1016/j.scitotenv.2021.148082
Cazenave A, Cozannet GL (2014) Sea level rise and its coastal impacts. Earth's Future 2(2):15–34. https://doi.org/10.1002/2013EF000188
Ceia FR, Patrício J, Marques JC, Dias JA (2010) Coastal Vulnerability in Barrier Islands: The High Risk Areas of the Ria Formosa (Portugal) System. Ocean Coast Manag 53(8):478–486. https://doi.org/10.1016/j.ocecoaman.2010.06.004
Costas S, Ferreira O, Martinez G (2015) Why do we decide to live with risk at the coast? Ocean Coast Manag 118:1–11. https://doi.org/10.1016/j.ocecoaman.2015.05.015
Davies-Vollum KS, West M (2015) Shoreline Change and Sea Level Rise at the Muni-Pomadze Coastal Wetland (Ramsar site) Ghana. J Coast Conserv 19(4):515–525. https://doi.org/10.1007/s11852-015-0403-y
Defeo O, McLachlan A, Schoeman DS, Schlacher TA, Dugan J, Jones A, Lastra M, Scapini F (2009) Threats to Sandy Beach Ecosystems: A Review. Estuar Coast Shelf Sci 81(1):1–12. https://doi.org/10.1016/j.ecss.2008.09.022
Didier D, Baudry J, Bernatchez P, Dumont D, Sadegh M, Bismuth E, Bandet M, Dugas S, Sévigny C (2019) Multihazard simulation for coastal flood mapping: Bathtub versus numerical modelling in an open estuary, Eastern Canada. J Flood Risk Manag 12(S1). https://doi.org/10.1111/jfr3.12505
Domingues RB, Jesus SN, Ferreira Ó (2021) Place Attachment, Risk Perception, and Preparedness in a Population Exposed to Coastal Hazards: A Case Study in Faro Beach, Southern Portugal. Int J Dis Risk Reduct 60:102288. https://doi.org/10.1016/j.ijdrr.2021.102288
Donnelly, C. (2008. Coastal overwash: processes and modelling [Ph.D Thesis]. Lund University
Donnelly C, Wamsley TV, Kraus NC, Larson M, Hanson H (2006) Morphologic Classification of Coastal Overwash. In: Proceedings 30th Coastal Engineering Conference
Duarte CR, de Miranda FP, Landau L, Souto MVS, Sabadia JAB, Neto CÂ da S, Rodrigues LI de C, Damasceno AM (2018) Short-Time Analysis of Shoreline Based on RapidEye Satellite Images in the Terminal Area of Pecém Port, Ceará, Brazil. Int J Remote Sens 39(13):4376–4389. https://doi.org/10.1080/01431161.2018.1457229
El-Asmar HM, Taha MMN, El-Sorogy AS (2016) Morphodynamic Changes as an Impact of Human Intervention at the Ras El-Bar-Damietta Harbor coast, NW Damietta Promontory, Nile Delta, Egypt. J African Earth Sci 124:323–339. https://doi.org/10.1016/j.jafrearsci.2016.09.035
Elliott M, Day JW, Ramachandran R, Wolanski E (2019) A synthesis: what is the future for coasts, estuaries, deltas and other transitional habitats in 2050 and beyond? In Coasts and Estuaries (pp. 1–28). Elsevier. https://doi.org/10.1016/B978-0-12-814003-1.00001-0
English E, Klink N, Turner S (2016) Thriving with water: Developments in amphibious architecture in North America. E3S Web of Conferences 7:13009. https://doi.org/10.1051/e3sconf/20160713009
ESRI (2019) ArcGIS Desktop (10.8.0.12790) [Computer software]. ESRI Inc
Feagin RA, Lozada-Bernard SM, Ravens TM, Möller I, Yeager KM, Baird AH (2009) Does Vegetation Prevent Wave Erosion of Salt Marsh Edges? Proc Natl Acad Sci 106(25):10109–10113. https://doi.org/10.1073/pnas.0901297106
Ferreira Ó, Matias A, Pacheco A (2016) The East Coast of Algarve: A Barrier Island Dominated Coast. Thalassas: Int J Mar Sci 32(2):75–85. https://doi.org/10.1007/s41208-016-0010-1
Ferreira Ó, Plomaritis TA, Costas S (2019) Effectiveness Assessment of Risk Reduction Measures at Coastal Areas Using a Decision Support System: Findings from Emma Storm. Sci Total Environ 657:124–135. https://doi.org/10.1016/j.scitotenv.2018.11.478
Ferreira Ó, Kupfer S, Costas S (2021) Implications of Sea-Level Rise for Overwash Enhancement at South Portugal. Nat Hazards 109(3):2221–2239. https://doi.org/10.1007/s11069-021-04917-0
Fox-Kemper B, Hewitt HT, Xiao C, Aðalgeirsdóttir G, Drijfhout SS, Edwards TL, Golledge NR, Hemer M, Kopp RE, Krinner G, Mix A, Notz D, Nowicki S, Nurhati IS, Ruiz L, Sallée J-B, Slangen ABA, Yu Y (2021) Ocean,cryosphere and sea level change. In: Masson-Delmotte V, Zhai P, Pirani A, Connors SL, Péan C, Berger S, Caud N, Chen Y, Goldfarb L, Gomis MI, Huang M, Leitzell K, Lonnoy E, Matthews JBR, Maycock TK, Waterfield T, Yelekçi O, Yu R, Zhou B (eds) Climate change 2021: the physical science basis. contribution of workinggroup I to the sixth assessment report of the intergovernmental panel on climate change. Cambridge University Press,Cambridge and New York, NY, pp 1211–1362. https://doi.org/10.1017/9781009157896.011
Garcia T, Ferreira Ó, Matias A, Dias JA (2010) Overwash Vulnerability Assessment Based on Long-term Washover Evolution. Nat Hazards 54(2):225–244. https://doi.org/10.1007/s11069-009-9463-3
Garner GG, Hermans T, Kopp RE, Slangen ABA, Edwards TL, Levermann A, Nowikci S, Palmer MD, Smith C, Fox-Kemper B, Hewitt HT, Xiao C, Aðalgeirsdóttir G, Drijfhout SS, Edwards TL, Golledge NR, Hemer M, Kopp RE, Krinner G, Mix A, Notz D, Nowicki S, Nurhati IS, Ruiz L, Sallée J-B, Yu Y, Hua L, Palmer T, Pearson B (2021a) IPCC AR6 sea-level rise projections. Version 2021a0809. PO.DAAC, CA, USA. https://podaac.jpl.nasa.gov/announcements/2021-08-09-Sea-level-projections-from-the-IPCC-6th-Assessment-Report. Accessed 2021–12–03
Garner GG, Kopp RE, Hermans T, Slangen ABA, Koubbe G, Turilli M, Jha S, Edwards TL, Levermann A, Nowikci S, Palmer MD, Smith C (2021b) Framework for assessing changes to sea-level (FACTS). Geoscientific Model Development
Ghaderi D, Rahbani M (2020) Detecting shoreline change employing remote sensing images (Case Study: Beris Port - East of Chabahar, Iran). International Journal of Coastal and Offshore Engineering 3(4):1–8. https://doi.org/10.29252/ijcoe.3.4.1
Halpern BS, Selkoe KA, Micheli F, Kappel CV (2007) Evaluating and Ranking the Vulnerability of Global Marine Ecosystems to Anthropogenic Threats. Conserv Biol 21(5):1301–1315. https://doi.org/10.1111/j.1523-1739.2007.00752.x
Herbert D, Astrom E, Bersoza A, Batzer A, McGovern P, Angelini C, Wasman S, Dix N, Sheremet A (2018) Mitigating Erosional Effects Induced by Boat Wakes with Living Shorelines. Sustainability 10(2):436. https://doi.org/10.3390/su10020436
Hidroprojecto (2005) Estudo de Impacto Ambiental do Projecto do Porto de Abrigo para a Pequena Pesca na Ilha da Culatra (Resumo Não Técnico 01.RP-I.004(1)), p 23
Himmelstoss EA, Henderson RE, Kratzmann MG, Farris AS (2018) Digital shoreline analysis system (DSAS) version 5.0 user guide: U.S. Geologial Survey Open-File Report, 2018–1179, p 110. https://doi.org/10.3133/ofr20181179
Hsu T-W, Lin T-Y, Tseng I-F (2007) Human Impact on Coastal Erosion in Taiwan. J Coastal Res 234:961–973. https://doi.org/10.2112/04-0353R.1
IPCC (2021) Summary for Policymakers. In: Masson-Delmotte V, Zhai P, Pirani A, Connors SL, Péan C, Berger S, Caud N, Chen Y, Goldfarb L, Gomis MI, Huang M, Leitzell K, Lonnoy E, Matthews JBR, Maycock TK, Waterfield T, Yelekçi O, Yu R, Zhou B (eds) Climate change 2021: the physical science basis. Contribution of working group I to the sixth assessment report of the intergovernmental panel on climate change. Cambridge University Press, Cambridge and New York, NY p 3–32. https://doi.org/10.1017/9781009157896.001
Kombiadou K, Matias A, Carrasco AR, Ferreira Ó, Costas S, Vieira G (2018) Towards Assessing the Resilience of Complex Coastal Systems: Examples from Ria Formosa (South Portugal). J Coastal Res 85:646–650. https://doi.org/10.2112/SI85-130.1
Kombiadou K, Matias A, Ferreira Ó, Carrasco AR, Costas S, Plomaritis T (2019) Impacts of Human Interventions on the Evolution of the Ria Formosa Barrier Island System (S. Portugal). Geomorphology 343:129–144. https://doi.org/10.1016/j.geomorph.2019.07.006

Kulp SA, Strauss BH (2019) New elevation data triple estimates of global vulnerability to sea-level rise and coastal flooding. Nat Commun 10(1):4844. https://doi.org/10.1038/s41467-019-12808-z

Li X, Grady CJ, Peterson AT (2014) Delineating Sea Level Rise Inundation Using a Graph Traversal Algorithm. Mar Geodesy 37(2):267–281. https://doi.org/10.1080/01490419.2014.902884

Liao K-H, Le TA, Nguyen KV (2016) Urban design principles for flood resilience: Learning from the ecological wisdom of living with floods in the Vietnamese Mekong Delta. Landsc Urban Plan 155:69–78. https://doi.org/10.1016/j.landurbplan.2016.01.014

Lopes CL, Sousa MC, Ribeiro A, Pereira H, Pinheiro JP, Vaz L, Dias JM (2022) Evaluation of Future Estuarine Floods in a Sea Level Rise Context. Sci Rep 12:8083. https://doi.org/10.1038/s41598-022-12122-7

Mattheus CR, Diggins TP (2019) Geomorphology of a Harbor-Breakwater Beach along a High Sand-Supply, Wave-Dominated Great Lakes Littoral Cell. J Coastal Res 35(1):41. https://doi.org/10.2112/JCOASTRES-D-17-00209.1

Nave S, Rebêlo L (2021) Coastline Evolution of the Portuguese South Eastern Coast: A High-Resolution Approach in a 65 Years' Time-Window. J Coast Conserv 25(1):7. https://doi.org/10.1007/s11852-020-00791-3

Neumann B, Vafeidis AT, Zimmermann J, Nicholls RJ (2015) Future Coastal Population Growth and Exposure to Sea-Level Rise and Coastal Flooding—A Global Assessment. PLOS ONE 10(3):e0118571. https://doi.org/10.1371/journal.pone.0118571

Nienhuis JH, Lorenzo-Trueba J (2019) Simulating Barrier Island Response to Sea Level Rise with the Barrier Island and Inlet Environment (BRIE) Model v1.0. Geophysical Research Letters 12(9):4013–4030. https://doi.org/10.5194/gmd-12-4013-2019

Pacheco A, Vila-Concejo A, Ferreira Ó, Dias JA (2008) Assessment of Tidal Inlet Evolution and Stability Using Sediment Budget Computations and Hydraulic Parameter Analysis. Mar Geol 247(1–2):104–127. https://doi.org/10.1016/j.margeo.2007.07.003

Pacheco A, Ferreira Ó, Williams JJ (2011) Long-Term Morphological Impacts of the Opening of a New Inlet on a Multiple Inlet System. Earth Surf Proc Land 36(13):1726–1735. https://doi.org/10.1002/esp.2193

Pacheco A, Monteiro J, Santos J, Sequeira C, Nunes J (2021) Energy Transition Process and Community Engagement on Geographic Islands: The Case of Culatra Island (Ria Formosa, Portugal). Renew Energy 184:700–711. https://doi.org/10.1016/j.renene.2021.11.115

Perini L, Calabrese L, Salerno G, Ciavola P, Armaroli C (2016) Evaluation of Coastal Vulnerability to Flooding: Comparison of Two Different Methodologies Adopted by the Emilia-Romagna Region (Italy). Nat Hazard 16(1):181–194. https://doi.org/10.5194/nhess-16-181-2016

Pickering MD, Horsburgh KJ, Blundell JR, Hirschi JJ-M, Nicholls RJ, Verlaan M, Wells NC (2017) The Impact of Future Sea-Level Rise on the Global Tides. Cont Shelf Res 142:50–68. https://doi.org/10.1016/j.csr.2017.02.004

Pilkey OH, Monteiro JH, Dias JMA, Neal WJ (1989) Algarve Barrier Islands: A Noncoastal-Plain System in Portugal. J Coastal Res 5(2):239–261

Plomaritis TA, Ferreira Ó, Costas S (2018) Regional Assessment of Storm Related Overwash and Breaching Hazards on Coastal Barriers. Coast Eng 134:124–133. https://doi.org/10.1016/j.coastaleng.2017.09.003

Poulter B, Halpin PN (2008) Raster Modelling of Coastal Flooding from Sea-level Rise. Int J Geogr Inf Sci 22(2):167–182. https://doi.org/10.1080/13658810701371858

Proverbs D, Lamond J (2017) Flood resilient construction and adaptation of buildings. In: Proverbs D, Lamond J (eds) Oxford research encyclopedia of natural hazard science. Oxford University Press. https://doi.org/10.1093/acrefore/9780199389407.013.111

Prumm M, Iglesias G (2016) Impacts of port development on estuarine morphodynamics: Ribadeo(Spain). Ocean Coast Manag 130:58–72. https://doi.org/10.1016/j.ocecoaman.2016.05.003

Sakhaee F, Khalili F (2021) Sediment pattern & rate of bathymetric changes due to construction of breakwater extension at Nowshahr port. J Ocean Eng Sci 6(1):70–84. https://doi.org/10.1016/j.joes.2020.04.002

Salles P, Voulgaris G, Aubrey DG (2005) Contribution of Nonlinear Mechanisms in the Persistence of Multiple Tidal Inlet Systems. Estuar Coast Shelf Sci 65(3):475–491. https://doi.org/10.1016/j.ecss.2005.06.018

Sekovski I, Armaroli C, Calabrese L, Mancini F, Stecchi F, Perini L (2015) Coupling Scenarios of Urban Growth and Flood Hazards Along the Emilia-Romagna Coast (Italy). Nat Hazard 15(10):2331–2346. https://doi.org/10.5194/nhess-15-2331-2015

Sharma S, Goff J, Cebrian J, Ferraro C (2016) A hybrid shoreline stabilization technique: Impact of modified intertidal reefs on marsh expansion and nekton habitat in the northern Gulf of Mexico. Ecol Eng 90:352–360. https://doi.org/10.1016/j.ecoleng.2016.02.003

Shenghui J, Rijun H, Xiuli F, Longhai Z, Wei Z, Aijiang L (2018) Influence of the construction of the Yantai West Port on the dynamic sedimentary environment. Mar Georesour Geotechnol 36(1):43–51. https://doi.org/10.1080/1064119X.2017.1278809

Silveira F, Lopes CL, Pinheiro JP, Pereira H, Dias JM (2021) Coastal floods induced by mean sea level rise—ecological and socioeconomic impacts on a Mesotidal Lagoon. J Mar Sci Eng 9(12):1430. https://doi.org/10.3390/jmse9121430

Sistema Nacional de Informação Geográfica (2011) Modelo Digital do Terreno (Resolução 2 m) - Zonas Costeiras de Portugal Continental - 2011. https://dados.gov.pt/en/datasets/modelo-digital-do-terreno-resolucao-2-m-zonas-costeiras-de-portugal-continental-2011/#_

Song H, Kuang C, Liang H, Xie H (2017) Impacts of Construction of Harbor Projects on Hydrodynamic and Sediment Transport Environments in the Southwest of Bohai Bay. Journal of Tongji University, 45(4), 511–518. https://doi.org/10.11908/j.issn.0253-374x.2017.04.008

Terres de Lima L, Fernández-Fernández S, Gonçalves JF, Magalhães Filho L, Bernardes C (2021) Development of Tools for Coastal Management in Google Earth Engine: Uncertainty Bathtub Model and Bruun Rule. Remote Sens 13(8):1424. https://doi.org/10.3390/rs13081424

Vousdoukas MI, Voukouvalas E, Annunziato A, Giardino A, Feyen L (2016) Projections of Extreme Storm Surge Levels Along Europe. Clim Dyn 47(9–10):3171–3190. https://doi.org/10.1007/s00382-016-3019-5

Waltham NJ, Alcott C, Barbeau MA, Cebrian J, Connolly RM, Deegan LA, Dodds K, Goodridge Gaines LA, Gilby BL, Henderson CJ, McLuckie CM, Minello TJ, Norris GS, Ollerhead J, Pahl J, Reinhardt JF, Rezek RJ, Simenstad CA, Smith JAM, … Weinstein MP (2021) Tidal Marsh Restoration Optimism in a Changing Climate and Urbanizing Seascape. *Estuaries and Coasts*, *44*(6), 1681–1690. https://doi.org/10.1007/s12237-020-00875-1

Williams LL, Lück-Vogel M (2020) Comparative assessment of the GIS based bathtub model and an enhanced bathtub model for coastal inundation. J Coast Conserv 24(2):23. https://doi.org/10.1007/s11852-020-00735-x

Yincan Y (2017) Chapter 7 - coastal erosion. In Marine Geo-Hazards in China. Elsevier, pp 269–296. https://doi.org/10.1016/B978-0-12-812726-1.00007-3

Zhou Z, Liang M, Chen L, Xu M, Chen X, Geng L, Li H, Serrano D, Zhang H, Gong Z, Zhang C (2022) Processes, feedbacks, and morphodynamic evolution of tidal flat–marsh systems: progress and challenges. Water Sci Eng 15(2):89–102. https://doi.org/10.1016/j.wse.2021.07.002